European Journal of Pharmaceutical Sciences 82 (2016) 1–10

Contents lists available at ScienceDirect

European Journal of Pharmaceutical Sciences

journal homepage: www.elsevier.com/locate/ejps

Oral delivery of zoledronic acid by non-covalent conjugation with lysine-deoxycholic acid: In vitro characterization and in vivo anti-osteoporotic efficacy in ovariectomized rats

Ok-Cheol Jeon [a,1], Dong-Hyun Seo [b,c,1], Han-Sung Kim [b,c], Youngro Byun [d,*], Jin Woo Park [e,**]

[a] College of Pharmacy, Seoul National University, Seoul, Republic of Korea
[b] Department of Biomedical Engineering, College of Health Science, Yonsei University, Wonju, Gangwon, Republic of Korea
[c] Yonsei-Fraunhofer IZFP Medical Device Lab., Wonju, Gangwon, Republic of Korea
[d] Department of Molecular Medicine and Biopharmaceutical Science, Graduate School of Convergence Science and Technology, College of Pharmacy, Seoul National University, Seoul, Republic of Korea
[e] College of Pharmacy and Natural Medicine Research Institute, Mokpo National University, Muan-gun, Jeonnam, Republic of Korea

ARTICLE INFO

Article history:
Received 28 July 2015
Received in revised form 2 November 2015
Accepted 2 November 2015
Available online 2 November 2015

Keywords:
Zoledronic acid
Lysine-deoxycholic acid
Oral delivery
Osteoporosis
Oral absorption enhancer

ABSTRACT

We assessed the possibility of changing the route of administration of zoledronic acid to an oral dosage form and its therapeutic efficacy in an estrogen-deficient osteoporosis rat model. To enhance oral bioavailability, we formed an ionic complex by electrostatic conjugation of zoledronic acid with lysine-linked deoxycholic acid (Lys-DOCA, an oral absorption enhancer). After forming the complex, the characteristic crystalline features of pure zoledronic acid disappeared completely in the powder X-ray diffractogram and differential scanning calorimetry thermogram, indicating that zoledronic acid existed in an amorphous form in the complex. In vitro permeabilities of zoledronic acid/Lys-DOCA (1:1) (ZD1) and zoledronic acid/Lys-DOCA (1:2) (ZD2) complex across Caco-2 cell monolayers were 2.47- and 4.74-fold higher than that of zoledronic acid, respectively. Upon intrajejunal administration to rats, the intestinal absorption of zoledronic acid was increased significantly and the resulting oral bioavailability of the ZD2 complex was determined to be 6.76 ± 2.59% (0.548 ± 0.161% for zoledronic acid). Ovariectomized (OVX) rats showed 122% increased bone mineral density versus the OVX control at 12 weeks after treatment with once weekly oral administration of ZD2 complex (16 μg/kg of zoledronic acid). Furthermore, rats treated with ZD2 complex orally showed significant improvement in the parameters of trabecular microarchitecture and bone strength: 149% higher bone volume fraction (BV/TV), 115% higher trabecular number (Tb.N), and 56% higher mean maximum load (F_{max}) than in the OVX group. The trabecular microstructure and bone mechanical properties in the oral zoledronic acid group were not significantly changed compared with the OVX control. Thus, the oral ZD2 complex inhibited osteoporosis progression effectively by promoting osteogenesis and trabecular connectivity. The oral ZD2 complex would be expected to improve patient compliance by replacing the conventional injectable form and expand the indications, to include prophylaxis for osteoporosis and bone metastases.

1. Introduction

Zoledronic acid is a potent nitrogen-containing parenteral bisphosphonate, used clinically as an anti-resorptive agent in treating osteoporosis, Paget's disease, hypercalcemia, multiple myeloma, and bone metastases arising from solid tumors, such as breast, prostate, and lung cancers (Black et al., 2007; Boissier et al., 2000; Novartis Pharmaceutical Corp., 2003). The primary mode of action of zoledronic acid is inhibition of bone resorption via induction of osteoclast apoptosis (Green et al., 1994; Hornby et al., 2003). As is true of other bisphosphonates, zoledronic acid exhibits a high affinity for hydroxyapatite and binds directly to mineralized zones at sites of drug release. The drug then becomes internalized by osteoclasts that are engaging in bone resorption, compromising osteoclast formation, function, and survival. It also induces apoptosis of various types of cancer cells (Corey et al., 2003; Dunford et al., 2001; Khajuria et al., 2015).

Zoledronic acid is currently only available in a parental dosage form for infusion over at least 15 min (Novartis Pharmaceutical Corp., 2003). However, too rapid an injection of bisphosphonate can cause the formation of complexes with calcium in the blood, leading to renal failure due to the complex being retained in the kidney (Blanchette and Pritchard,

* Correspondence to: Y. Byun, College of Pharmacy, Seoul National University, 1 Gwanak-ro, Gwanak-gu, Seoul 151-742, Republic of Korea
** Correspondence to: J. W. Park, College of Pharmacy, Mokpo National University, 1666 Youngsan-ro, Muan-gun, Jeonnam 534-729, Republic of Korea.
E-mail addresses: yrbyun@snu.ac.kr (Y. Byun), jwpark@mokpo.ac.kr (J.W. Park).
[1] Ok-Cheol Jeon and Dong-Hyun Seo equally contributed as first authors to this work.

http://dx.doi.org/10.1016/j.ejps.2015.11.004
0928-0987/

2015). Moreover, local delivery of bisphosphonates, such as subcutaneous or intramuscular administration increases the risk of tissue irritation, inflammation, pain, and necrosis at the injection site (Ezra and Golomb, 2000; Lin, 1996). Given this background, there is a demand for the development of other dosage forms of zoledronic acid, particularly an oral dosage form, because orally administered drugs are becoming more widespread in many therapeutic areas, including the treatment of cancer.

However, all bisphosphonates, including zoledronic acid, exhibit low oral bioavailability (<1%), attributable to the drugs being highly polar and hydrophilic and the fact that they form insoluble metal complexes in the upper intestine, most commonly with calcium, resulting in low gastrointestinal (GI) permeation (Lin, 1996). For these reasons, oral delivery of zoledronic acid has been challenging. There have been various attempts to generate novel oral formulations by crystallization and the formation of metal salts, including Na^+, Ca^{2+}, Mg^{2+}, Zn^{2+}, mono- and trihydrates, and amorphous forms of zoledronic acid, to improve its aqueous solubility, permeability, and subsequent oral bioavailability (Aronhime et al., 2005; Mohakhud et al., 2006; Novartis Ag et al., 2008). Additionally, Merrion Pharmaceuticals prepared an oral dosage form of zoledronic acid wherein a medium chain fatty acid or a salt of a medium chain fatty acid having a carbon chain length of 6–20 carbon atoms was used as an oral enhancer (Merrion Research Ill Ltd., 2010) and Thar Pharmaceuticals used modified amino acid carriers by complex formation with amino acids to enhance the oral absorption of zoledronic acid (Thar Pharmaceuticals, Inc., 2011).

In a previous study, we have shown that the intestinal permeability of bisphosphonates such as ibandronate could be significantly improved by generation of molecular complexes with lysine-linked deoxycholic acid (Lys-DOCA) (Park et al., 2013). The aim of the current study was to expand our technology to develop an oral formulation of zoledronic acid, resulting in a new dosage form for long-term administration by conjugating the Lys-DOCA as an absorption enhancer to increase the intestinal permeability and prove its therapeutic efficacy in vivo. After characterization of the zoledronic acid/Lys-DOCA (ZD) complexes in terms of crystallinity and water solubility, we confirmed the in vitro drug permeability through an artificial intestinal membrane and a Caco-2 cell monolayer, followed by assessment of the oral bioavailability of the ZD complex in vivo. Finally, the ZD complex was administered orally to ovariectomized (OVX) rats once per week, after which we evaluated its anti-osteoporotic efficacy compared with oral or intraperitoneally injected zoledronic acid by analyzing bone properties, such as bone mineral density (BMD), trabecular bone microarchitecture in tibiae, and biomechanical strength.

2. Materials and methods

2.1. Materials

Zoledronic acid was obtained as the hydrated disodium salt from Ultratech India Ltd. (Mumbai, India). Deoxycholic acid (DOCA), ethyl chloroformate, N-methylmorpholine, N_ε-Boc-L-lysine methyl ester hydrochloride (H-Lys(Boc)-OMe·HCl), lithium aluminum hydride ($LiAlH_4$), ibandronate, trimethylsilyl diazomethane (TMSD; 2 M solution in hexane), ammonium acetate, and formic acid were purchased from Sigma-Aldrich Co. (St. Louis, MO, USA). Tetrahydrofuran (THF), chloroform, methanol, acetyl chloride, and *n*-hexane (analytical grade) were obtained from Merck Co. (Darmstadt, Germany). Solvents for high-performance liquid chromatography (HPLC) and liquid chromatography/tandem mass spectrometry (LC/MS/MS) analyses were from Merck KGaA (Darmstadt, Germany) and Fisher Scientific (Pittsburgh, PA, USA).

2.2. Animals

Sprague Dawley rats (females, 200–250 g) were purchased from Orient Co., Ltd. (Gyunggi-do, Republic of Korea). The animals were acclimated for 1 week in an animal facility under controlled conditions of temperature (23 ± 2 °C), relative humidity (55 ± 10%), and light (12/12-h light/dark, with no ultraviolet exposure). The animals had free access to a laboratory diet (Purina Co., St. Louis, MO, USA) and ion-sterilized tap water.

The animal studies were approved by the Institutional Animal Care and Use Committee (IACUC) of Seoul National University (Seoul, Republic of Korea; approval date, 12/10/2014; ref. no., SNU-13081-3-1). All experiments were performed in accordance with the NIH guidelines for the Care and Use of Laboratory Animals and the guidelines of the IACUC.

2.3. Preparation of zoledronic acid/absorption enhancer complex

The oral absorption enhancer, N^α-deoxycholyl-L-lysyl-methylester (Lys-DOCA), was synthesized by conjugating DOCA with L-lysine, as described previously (Park et al., 2013). Briefly, ethyl chloroformate (6.4 mL) and N-methylmorpholine (7.4 mL) were dropped into 3.25% (w/v) DOCA solution in THF in an ice bath, and stirred for 30 min. Next, H-Lys(Boc)-OMe·HCl (20 g) and N-methylmorpholine (7.4 mL) were added to the mixture at room temperature, and the reaction mixture was refluxed for 2 h. After cooling to room temperature, the mixture was stirred overnight. The precipitates were filtered and the solvent was evaporated. Lys(Boc)DOCA was obtained by purification of the residue using column chromatography (chloroform/methanol). Lys(Boc)DOCA was dissolved in a solvent mixture of acetyl chloride (23.4 mL) and methanol (100 mL) in an ice bath and stirred for 30 min. After solvent evaporation, the residue was dissolved in water and washed with chloroform three times. Finally, the aqueous layer was lyophilized and Lys-DOCA was obtained as a white powder.

The ZD complex was prepared by the ionic interaction of zoledronic acid and Lys-DOCA under aqueous conditions. Briefly, 5 mg/mL solutions of zoledronic acid and Lys-DOCA were prepared separately in distilled water, and the ZD complex was then formed by the addition of Lys-DOCA solution into a zoledronic acid aqueous solution with continuous stirring. The complexation molar ratios of zoledronic acid to Lys-DOCA were 1:1 (ZD1) and 1:2 (ZD2). The solutions were then centrifuged and lyophilized at −80 °C to obtain white powders.

2.4. Characterization of zoledronic acid/absorption enhancer complex

Complex formation between zoledronic acid and Lys-DOCA was confirmed by comparing the characteristic crystalline features of pure zoledronic acid, Lys-DOCA, physical mixtures of zoledronic acid and Lys-DOCA, and the ZD complexes using powder X-ray diffraction (PXRD) and differential scanning calorimetry (DSC). PXRD patterns were collected with a Rigaku-D/MAX-IIIV diffractometer (D5005, Bruker, Germany) at 40 mA and 40 kV using Ni-filtered Cu-Kα radiation. The powdered samples were deposited on an adhesive support, 0.5 mm thick, and placed in the diffractometer. PXRD patterns were recorded in step-scan mode in the range $3° \le 2\theta \le 40°$ with a scanning rate of $0.02°s^{-1}$.

Thermal analysis of the samples was carried out using a DSC 204A/G Phoenix Instrument (Netzsch, Germany). Approximately 5 mg of each sample were weighed into a non-hermetically sealed aluminum pan and scanned at a heating rate of 5 °C/min over a temperature range of 25–250 °C. All DSC measurements were made under a nitrogen atmosphere at a flow rate of 100 mL/min.

2.5. Solubility and partition coefficient of the zoledronic acid/absorption enhancer complex

The solubilities of the ZD1 and ZD2 complexes in phosphate-buffered saline (PBS, pH 6.8) were determined. Briefly, excess ZD1 or ZD2 complex was added to 5 mL of PBS at pH 6.8 in a sealed glass container. The samples were agitated at 100 rpm for 24 h in a shaking water

bath at 37 °C and then centrifuged at 10,000 rpm for 10 min (Jena et al., 2014). The supernatant was filtered through a 0.45-μm membrane filter and analyzed by HPLC using a C18 column (5 μm, 100 Å, 4.6 × 250 mm; 20-μL sample injection) at 50 °C. The mobile phase, a mix of buffer (4.5 g potassium phosphate dibasic, 2.0 g tetrabutylammonium sulfate, and 1 L water) and acetonitrile (90:10, v/v), was run at a flow rate of 1.0 mL/min. Zoledronic acid or ZD complexes were detected using a UV detector at 215 nm. The partition coefficients (log P) of zoledronic acid and ZD complexes were determined by the shake-flask method after allowing *n*-octanol and PBS (pH 6.8) to equilibrate for 24 h at 25 °C. Zoledronic acid or ZD complexes (equivalent to 20 mg zoledronic acid) were added to 5 mL of PBS (pH 6.8) and agitated at 100 rpm for 24 h in a shaking water bath at 25 °C. Then, 5 mL of *n*-octanol were added as the non-aqueous phase, and the resulting solution was agitated for 24 h at 100 rpm and 25 °C. The aqueous and *n*-octanol phases were separated and centrifuged at 10,000 rpm for 15 min. The aqueous phase was extracted and the concentration of zoledronic acid was estimated using the HPLC system with a UV detector as described above. Log P was calculated using the following formula: log P = log (concentration in *n*-octanol/concentration in PBS at pH 6.8) (Ziemba et al., 2011).

2.6. In vitro permeability study

A parallel artificial membrane permeability assay (PAMPA, BD Biosciences, Bedford, MA, USA) was conducted according to the following protocol. A 96-well microtiter plate served as the receiving chamber and a 96-well microfilter plate served as the donor compartment. Zoledronic acid and ZD complexes were dissolved in PBS (pH 7.4). Then, 300 μL of the solution (equivalent to 200 μM zoledronic acid) were added to each donor plate well, and buffer (PBS, pH 7.4, 200 μL) was added to each well of the receptor plate. The filter (donor) plate was then coupled with the receiver plate and the plate assembly was incubated at room temperature for 5 h. After incubation, the concentration of zoledronic acid or ZD complex in the samples from the donor and receptor wells of the PAMPA was quantified by HPLC with a UV detector, as described above. The permeability of the compounds was calculated using the following formula:

$$P_e = \frac{-\ln\left[1 - \frac{C_A(t)}{C_{equilibrium}}\right]}{A \times \left(\frac{1}{V_D} + \frac{1}{V_A}\right) \times t}$$

where P_e is the permeability (cm/s); A is the effective filter area ($f \times 0.3$ cm^2), where f means the apparent porosity of the filter (f = 0.76); V_D is the donor well volume (0.3 mL); V_A is the receptor well volume (0.2 mL);. t is the incubation time (s); $C_A(t)$ indicates the concentration of compound in receptor well at time t; $C_D(t)$ indicates the concentration of compound in donor well at time t; and $C_{equilibrium}$ means $[C_D(t) \times V_D + C_A(t) \times V_A]/(V_D + V_A)$.

The in vitro permeability of zoledronic acid and ZD complexes across a Caco-2 cell monolayer was also investigated. The transport assay was performed as described by Hubatsch et al., 2007. In brief, the complete medium was removed from both the apical and basolateral compartments after culturing in a 12-well Transwell and the monolayer was pre-incubated with 0.5 mL of Hanks' balanced salt solution (HBSS) for 30 min at 37 °C. The medium was then removed from both compartments and 0.5 mL of zoledronic acid or ZD complex solution in HBSS (200 μM) was introduced to the apical side. Next, 1.5 mL of blank HBSS was added to the basolateral side. At predetermined times, the apical compartment was moved to another basolateral compartment containing 1.5 mL of fresh blank HBSS. The concentration of zoledronic acid or ZD complexes permeated though the monolayer was determined using the HPLC system with a UV detector, as described above. The apparent permeability coefficient (P_{app}) of zoledronic acid or ZD complex was calculated according to the following equation:

$$P_{app} = dQ/dt \times 1/(A \cdot C_0)$$

where dQ/dt indicates the linear appearance rate of mass in the basolateral sides (μmoL/s), C_0 is the initial concentration of zoledronic acid or ZD complex on the apical side (μM), and A is the surface area of the monolayer (cm^2).

2.7. Pharmacokinetic study in rats

Twelve female Sprague Dawley rats were used in this pharmacokinetic study. All animals were anesthetized with ketamine (45 mg/kg) and xylazine (5 mg/kg) by intramuscular injection. In eight rats, a midline abdominal incision was made to take out the small intestine and locate the injection site at the beginning of the jejunum, ~2 cm after the ligament of Treitz. Then the rats were divided into two groups (n = 4/group) and each animal received 400 μL solution intra-jejunally, consisting of zoledronic acid (5 mg/kg) or ZD2 (equivalent to 5 mg/kg zoledronic acid). Next, the intestines were carefully returned to the abdominal cavity (Cetin et al., 2008). To evaluate bioavailability, 150 μL zoledronic acid (1 mg/kg) in water was also prepared and injected via the tail vein (n = 4). After administration, blood samples (100 μL) were collected from a capillary from the retro orbital plexus and mixed directly with 10 μL of sodium citrate (3.8% solution). The blood samples were then immediately centrifuged (2500 × g, 15 min, 4 °C). Plasma samples were isolated and stored at − 70 °C until analysis.

To determine the plasma concentration of zoledronic acid, 50 μL of each standard and plasma sample were mixed with 5 μL of 40 μg/mL internal standard (IS, ibandronate) solution and 50 μL of 10 mM sodium bicarbonate solution. After vortexing for 5 s, an aliquot of the solution (100 μL) was loaded onto a solid-phase extraction cartridge that had been previously conditioned with methanol (1 mL) and deionized water (1 mL). Next, 100 μL of derivatization reagent, 1.0 M TMSD in hexane, was added to each cartridge and allowed to react with the analytes for 30 min. The derivatization reagent was then re-eluted from the cartridge under gravity and the cartridge was subsequently rinsed with methanol (1.5 mL). The collected methanol extracts were evaporated under nitrogen at 50 °C. The dried residues were reconstituted in 150 μL of acetonitrile-5 mM ammonium formate (50:50, v/v), followed by vortex mixing and centrifugation (3000 rpm, 1 min). An Acquity UPLC system (Waters, Milford, MA, USA) was used for the LC/MS/MS analysis, and the separation was carried out using a Luna 5-μm SCX 100-Å column (50 × 2.0 mm i.d.) with a mobile phase consisting of 5 mM ammonium formate buffer (pH 3.5, adjusted with formic acid)-acetonitrile (50:50, v/v) at a flow rate of 0.3 mL/min. The analytes were detected in the positive ion mode using a Finnigan TSQ Quantum Ultra (Thermo Scientific, Rockford, IL, USA) with a TurboIonSpray (ESI) source and quantitative determinations were performed in multiple reaction monitoring scan mode using the following transitions: m/z 329 → 125 for the zoledronic acid derivative and m/z 376 → 114 for the ibandronate derivative.

2.8. Anti-osteoporosis effect in OVX rats

To evaluate the anti-osteoporotic effects of the orally administered zoledronic acid and the Lys-DOCA complex in an OVX rat model, 40 female Sprague Dawley rats (8 weeks old) were used. Of them, 32 underwent bilateral ovariectomy to induce osteoporosis and 8 underwent sham surgeries (SHAM). After 2 weeks, the OVX rats were randomly divided into four groups of eight animals each: OVX (not treated), OVX-ZOL-IP (once weekly intraperitoneal injection of 1.6 μg/kg zoledronic acid), OVX-ZOL-ORAL (once weekly oral administration of 16 μg/kg zoledronic acid), and OVX-ZD2-ORAL (once weekly oral administration of ZD2 complex as 16 μg/kg zoledronic acid) groups.

During treatment, body weights were measured and the drug dose was adjusted. At 12 weeks after treatment, the tibiae were isolated from both legs of the rats and fixed in 4% formalin in PBS at pH 7.4 (Perilli et al., 2010).

2.8.1. Micro-computed tomography (μCT) scanning of tibia

To measure the BMD and explore the microarchitectural properties of trabecular bone, we performed histomorphometric analyses using a Skyscan 1076 in vivo micro-CT scanner (Bruker Corporation, Karlsruhe, Germany). Two-dimensional (2D) projections were obtained using an X-ray source setting of 70 kV and a current of 139 μA, with filtration of the beam through a 1.0-mm aluminum filter. Data were collected every at 0.5° of rotation from 0° through 180°. The scanning width was 35 mm and the height 17 mm. Three-dimensional (3D) microstructural images were reconstructed with the aid of a modified Feldkamp back-projection algorithm. The resulting raw image data were Gaussian filtered and subjected to global thresholding at a cross-section of 0.0 to 0.0752. Image conversion was then performed to extract the mineral phase. Using transverse image slices, the trabecular bone was segmented from the cortical bone using Skyscan CT-Analyzer software featuring semi-automated contouring. The BMD was measured in the midshaft region located one-quarter of the distance from the proximal tibial growth plate. To allow detailed qualitative and quantitative evaluation, the region scanned was confined to the distal metaphysis of the tibia, extending 1.0 mm proximally from the proximal growth plate. The following morphometric parameters were calculated: bone volume fraction (BV/TV), bone surface/volume ratio (BS/BV), trabecular thickness (Tb.Th), trabecular separation (Tb.Sp), trabecular pattern factor (Tb.Pf), trabecular number (Tb.N), and the structural model index (SMI).

2.8.2. Bone mechanical test

The mechanical properties of each tibia were assessed by three-point bending tests using a universal testing machine (BISS Makron, Bangalore, India). After measuring the length of the tibia using calipers, the bone was placed on a special holding device with two lower support bars located 15 mm apart in a repeated position. A bending force was applied with a crosshead speed of 1 mm/min until breakage. From the test data, the load–displacement curve for each sample in a group was plotted. Several biomechanical characteristics were determined from these curves, such as ultimate load at failure (the maximum force that the bone withstood before fracture, F_{max}) and stiffness (the extrinsic rigidity of the tibia before fracture).

2.8.3. Histological observation of tibiae

The fixed tibia tissues were decalcified with 10% EDTA, and dehydrated through a graded ethanol series. They were then embedded in paraffin wax, sectioned at 5 μm, and stained with hematoxylin and eosin (H&E) for standard evaluation. To evaluate osteoclast activity, the tibia bone sections were deparaffinized and then incubated in the tartrate-resistant acid phosphatase (TRAP) reagent for 1 h. After washing with distilled water, the sections were counterstained with 1% methyl green. The proximal part of the tibia was then observed under a light microscope (Bx-41; Olympus, Japan), and a photograph was taken while focusing on a central part of the growth plate.

2.9. Pharmacokinetic and statistical analyses

Pharmacokinetic parameters were obtained using a non-compartmental method in WinNonlin® software (ver. 5.3; Pharsight Corporation, Mountain View, CA). All data are expressed as means ± standard deviations. A p-value of <0.05 was considered to indicate statistical significance using a t-test between two mean values for unpaired data or two-way analysis of variance (ANOVA) followed by Tukey's multiple comparison tests among more than three mean values for unpaired data.

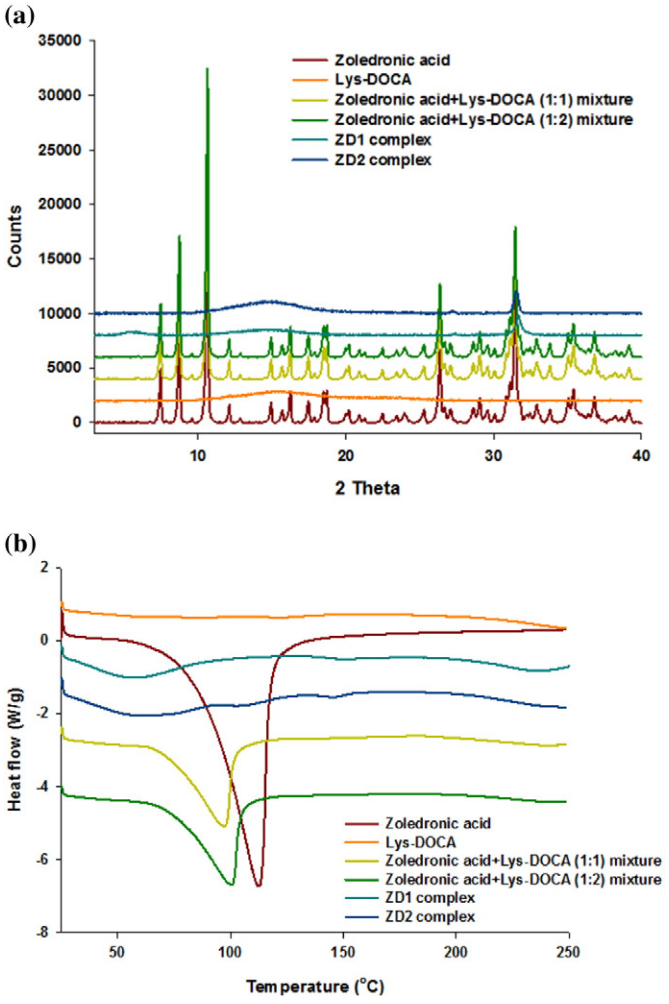

Fig. 1. (a) Powder X-ray diffractograms (PXRD) of zoledronic acid, lysine-linked deoxycholic acid (Lys-DOCA), 1:1 physical mixture of zoledronic acid and Lys-DOCA, 1:2 physical mixture of zoledronic acid and Lys-DOCA, zoledronic acid/Lys-DOCA (1:1) (ZD1) complex, and zoledronic acid/Lys-DOCA (1:2) (ZD2) complex. (b) Differential scanning calorimetry (DSC) thermograms of zoledronic acid, Lys-DOCA, 1:1 physical mixture of zoledronic acid and Lys-DOCA, 1:2 physical mixture of zoledronic acid and Lys-DOCA, zoledronic acid/Lys-DOCA (1:1) (ZD1) complex, and zoledronic acid/Lys-DOCA (1:2) (ZD2) complex.

3. Results

3.1. Characterization of zoledronic acid/Lys-DOCA complex

To identify the final solid state of the zoledronic acid, the PXRD spectra of the zoledronic acid, Lys-DOCA, and the physical mixtures were compared with that of the ZD complex (Fig. 1(a)). Pure zoledronic acid showed diffraction peaks at 7.48°, 8.74°, 10.64°, 26.36°, and 31.47° over the 2θ range in the PXRD spectra, characteristic peaks of crystalline zoledronic acid. In the physical mixture, zoledronic acid characteristic peaks were also clearly evident, indicating that the drug was

Table 1
Solubility in buffer and log P in n-octanol-buffer of zoledronic acid and zoledronic acid/Lys-DOCA (ZD) complexes.

Test material	Solubility (mg/mL)	Log P
Zoledronic acid	>290[a]	−0.985 ± 0.014
ZD1 complex	38.6 ± 2.69	−0.916 ± 0.012
ZD2 complex	30.4 ± 4.10	0.966 ± 0.008

[a] Data obtained from Zometa® [package insert]. Each value represents the mean ± standard deviation ($n = 4$).

Table 2
In vitro permeabilities of zoledronic acid and zoledronic acid/Lys-DOCA (ZD) complexes.

	Permeability (P_e, cm/s)[a]	Apparent permeability (P_{app}, cm/s)[b]
Zoledronic acid	N.D.[c]	2.72 ± 0.868 ($\times 10^{-6}$)
ZD1 complex	0.250 ± 0.242 ($\times 10^{-6}$)[d]	6.72 ± 1.94 ($\times 10^{-6}$)[e]
ZD2 complex	1.12 ± 0.144 ($\times 10^{-6}$)[e,g]	12.9 ± 3.11 ($\times 10^{-6}$)[e,f]

[a] Permeability coefficient (P_e) of zoledronic acid or ZD complex evaluated by a parallel artificial membrane permeability assay (PAMPA).
[b] Apparent permeability coefficient (P_{app}) of zoledronic acid or ZD complex through a Caco-2 cell monolayer.
[c] Not detected. Each value represents the mean ± standard deviation ($n = 6$).
[d] $p < 0.05$, compared to zoledronic acid.
[e] $p < 0.001$, compared to zoledronic acid.
[f] $p < 0.01$, compared to the ZD1 complex.
[g] $p < 0.001$, compared to the ZD1 complex.

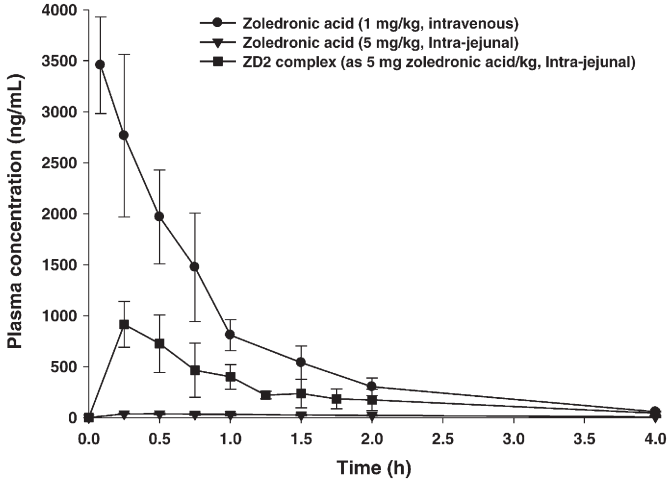

Fig. 2. Venous plasma concentration-time profiles of zoledronic acid after single intravenous administration of zoledronic acid (1 mg/kg), and intra-jejunal administration of zoledronic acid or zoledronic acid/Lys-DOCA (1:2) (ZD2) complex (equivalent to 5 mg/kg of zoledronic acid) to rats. Each value represents the mean ± standard deviation ($n = 4$).

still in crystalline form. However, no sharp diffraction peak of crystalline zoledronic acid was observed in the lyophilized ZD complexes. From the PXRD spectra, it can be concluded that the ionic complex formation of zoledronic acid with Lys-DOCA caused the dispersion of each material and amorphous zoledronic acid was formed.

The disappearance of crystallinity of zoledronic acid was also confirmed by DSC analysis (Fig. 1(b)). The characteristic endothermic peaks at 135 °C, 98 °C, and 101 °C were visible in the thermograms of both the crude zoledronic acid and physical mixtures, while they were absent in the DSC thermograms of the ZD complexes. Thus, it was concluded that the zoledronic acid was dispersed molecularly with Lys-DOCA and existed in an amorphous form after complex formation.

3.2. Solubility and partition coefficient of the zoledronic acid/Lys-DOCA complex

Although zoledronic acid is a very hydrophilic drug, with a solubility of more than 290 mg/mL at pH 6.8, the solubilities of the ZD1 and ZD2 complexes in PBS at pH 6.8 were 38.6 ± 2.69 and 30.4 ± 4.10 mg/mL, respectively (Table 1). Furthermore, zoledronic acid exhibited a very low partition coefficient (log P = −0.985 ± 0.014). However, its partition coefficient was significantly increased in the presence of Lys-DOCA and the log P value of the ZD2 complex was about 89.3-fold higher than that of zoledronic acid.

3.3. In vitro permeability study

In the in vitro artificial intestinal membrane permeability study, zoledronic acid did not completely pass through the artificial membrane, but the permeabilities of the ZD1 and ZD2 complexes were 0.250 ± 0.242 ($\times 10^{-6}$) and 1.12 ± 0.144 ($\times 10^{-6}$) cm/s, respectively (Table 2). Additionally, the permeability of zoledronic acid dissolved in the control buffer (HBSS) across a Caco-2 cell monolayer showed 2.27 ± 0.868 ($\times 10^{-6}$) cm/s. However, Lys-DOCA-conjugated zoledronic acid showed significantly increased apparent permeability. The P_{app} values for ZD1 and ZD2 were 6.72 ± 1.94 ($\times 10^{-6}$) cm/s and 12.9 ± 3.11 ($\times 10^{-6}$) cm/s, respectively, which are 2.47- and 4.74-fold higher, respectively, than that of zoledronic acid (Table 2). Generally, substances with an apparent permeability coefficient of $<1 \times 10^{-6}$ cm/s are classified as low-permeability substances, and high-permeability substances exhibit an apparent permeability coefficient of $>1 \times 10^{-5}$ cm/s (Spernath et al., 2007; Stenberg et al., 2001). Thus, the permeability of zoledronic acid was enhanced significantly by complex formation with Lys-DOCA and increased as the complexation molar ratio of Lys-DOCA increased.

3.4. In vivo pharmacokinetic properties of zoledronic acid and ZD complex

The in vitro permeability study showed that the ZD2 complex had a significantly higher permeability than zoledronic acid or the ZD1 complex ($p < 0.001$, except for the apparent permeability across a Caco-2 cell monolayer compared to the ZD1 complex, where $p = 0.002$). Therefore, further in vivo pharmacokinetic studies were performed using zoledronic acid and the ZD2 complex. Fig. 2 illustrates the change in the mean plasma concentrations of zoledronic acid after intra-jejunal administration of zoledronic acid or the ZD2 complex, and intravenous injection of zoledronic acid to rats. The intestinal absorption of zoledronic acid was significantly enhanced by complex formation with Lys-DOCA; the C_{max} of the ZD2 complex was 23.7-fold higher than that of

Table 3
Pharmacokinetic parameters after intra-jejunal administration of zoledronic acid or zoledronic acid/Lys-DOCA (1:2) complex.

Test material	Zoledronic acid	Zoledronic acid	Zoledronic acid/Lys-DOCA (1:2) complex
Administration	Intravenous	Intra-jejunal	Intra-jejunal
Dose of zoledronic acid (mg/kg)	1	5	5
T_{max} (h)[a]		0.500 ± 0.250	0.313 ± 0.125
C_{max} (ng/mL)[b]	3457 ± 474.2	38.66 ± 6.482	915.8 ± 222.1
AUC_{last} (ng · h/mL)[c]	3016 ± 691.6	82.66 ± 24.35	1020 ± 390.0
AUC_{inf} (ng · h/mL)[d]	3098 ± 673.5	104.7 ± 22.91	1090 ± 399.5
Bioavailability (%)[e]	100	0.548 ± 0.161	6.76 ± 2.59

[a] T_{max}, time to reach C_{max}.
[b] C_{max}, maximum plasma concentration.
[c] AUC_{last}, area under the plasma concentration-time curve from zero to the time of the last measurable plasma concentration.
[d] AUC_{inf}, area under the plasma concentration-time curve from zero to infinity.
[e] Bioavailability, $(AUC_{last,\ intra\text{-}jejunal} / Dose_{zoledronic\ acid,\ intra\text{-}jejunal}) / (AUC_{last,\ intravenous} / Dose_{zoledronic\ acid,\ intravenous}) \times 100$. Each value represents the mean ± standard deviation ($n = 4$).

zoledronic acid (38.66 ± 6.482 ng/mL). The AUC_{last} value of the ZD2 complex increased by 12.3-fold compared with that of zoledronic acid (82.66 ± 24.35 ng · h/mL). The resulting oral bioavailability of the ZD2 complex was determined to be 6.76 ± 2.59% (0.548 ± 0.161% for zoledronic acid); it improved significantly due to complex formation with Lys-DOCA (Table 3).

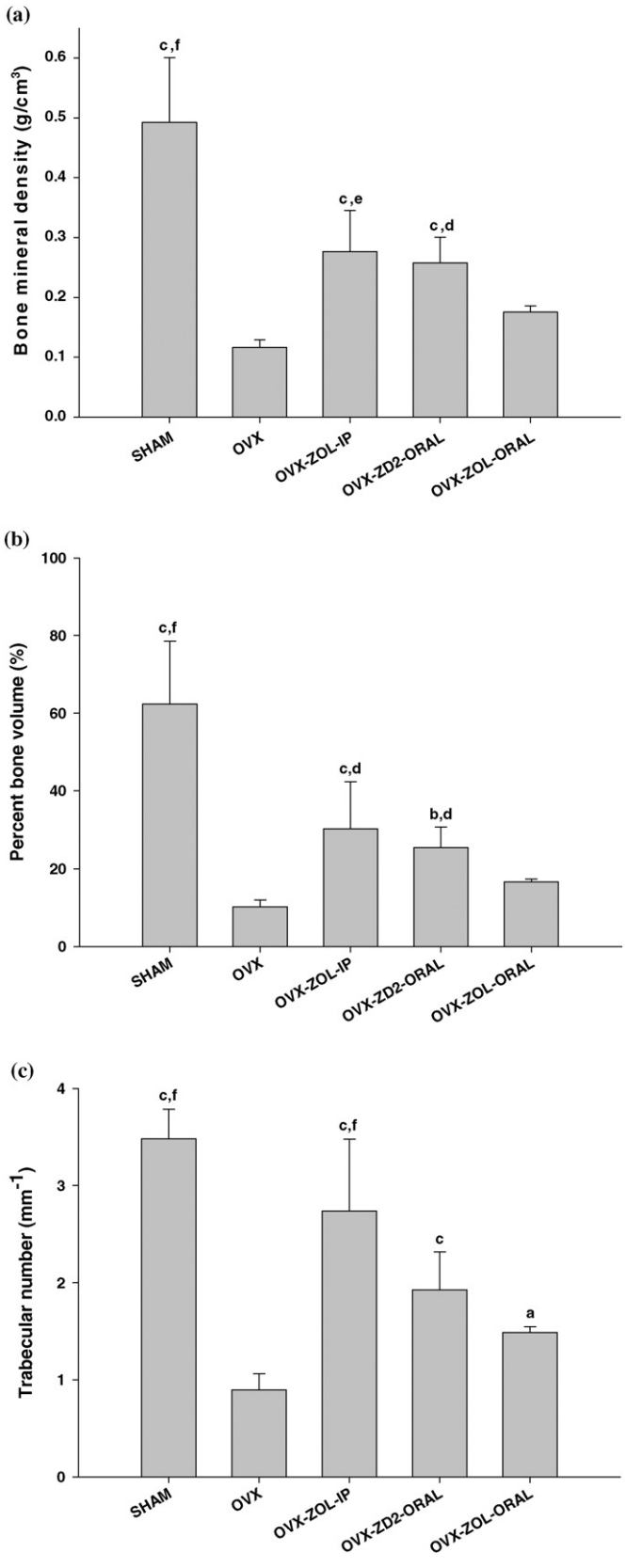

3.5. In vivo anti-osteoporotic effects of orally administered ZD complex

To evaluate the anti-osteoporotic effects of oral administration of the ZD2 complex on the estrogen-deficient osteoporosis-induced rat model, BMD in the tibiae was analyzed. The final body weights of rats in all OVX groups were increased significantly compared with those in the SHAM group. As shown in Fig. 3(a), the BMD values of tibiae in groups treated with weekly intraperitoneal injection of zoledronic acid or oral administration of ZD2 complex were significantly higher than that of the OVX control group. Compared with the OVX group, OVX-ZOL-IP and OVX-ZD2-ORAL showed 138% and 122% increases in BMD, respectively. However, the OVX-ZOL-ORAL revealed no significant improvement in BMD compared with the OVX.

The results from evaluation of the trabecular bone microarchitecture in the tibia metaphyseal region using μCT are listed in Table 4. After a 12-week treatment, the SHAM group showed significantly improved morphological parameters versus the OVX group: 511% greater BV/TV and 288% greater Tb.N. This indicated increased bone mass, accompanied by a transition from a merely rod-like structure to an almost plate-like structure. Conversely, the OVX group exhibited dramatic bone loss after 14 weeks. The OVX-ZOL-IP group showed 197% and 205% higher BV/TV and Tb.N, respectively, versus the OVX group. Moreover, the OVX-ZD2-ORAL group showed significant improvement in structural parameters: 149% higher BV/TV and 115% higher Tb.N as compared to the OVX group. However, the OVX-ZOL-ORAL group showed 66% higher Tb.N than the OVX group, but the levels of all other parameters did not significantly change. Compared with the OVX-ZOL-ORAL group, BV/TV and Tb.N were 83% and 84% higher in the OVX-ZOL-IP group, respectively, and the OVX-ZD2-ORAL group exhibited a 53% higher BV/TV (Fig. 3(b) and (c)).

Fig. 4 shows representative 2D and 3D μCT reconstruction images of the tibia bone. Deterioration of the trabecular microarchitecture in tibia bone was readily observed in the OVX group, compared with numerous and well-developed trabeculae in the SHAM group. However, the OVX-ZOL-IP and OVX-ZD2-ORAL groups presented tighter and denser structures compared with the OVX-ZOL-ORAL and OVX groups, providing evidence of improvements in the trabecular microarchitecture of the proximal tibia.

3.6. Biomechanical tests

The F_{max} and stiffness evaluated by three-point bending tests of the tibia in each group are shown in Fig. 5. The bone mechanical strength parameters were reduced significantly by ovariectomy; the F_{max} and stiffness in the OVX group were decreased by 54% and 51%, respectively, compared with the SHAM group (F_{max}: 109.5 ± 24.13 N; stiffness: 167.1 ± 19.61 N/m). However, the F_{max} and stiffness were significantly greater in both the OVX-ZOL-IP group (F_{max}: 85.27 ± 9.450 N; stiffness: 133.5 ± 20.10 N/m, +63%) and the OVX-ZD2-ORAL group (F_{max}: 77.75 ± 7.180 N, +56%; stiffness: 117.3 ± 15.96 N/m, +43%) than

Fig. 3. Micro-computed tomography (μCT) analyses of tibiae of rats that were either sham-operated (SHAM) or ovariectomized (OVX) and treated with once-weekly intraperitoneal injection of 1.6 μg/kg zoledronic acid (OVX-ZOL-IP), or once-weekly oral administration of 16 μg/kg zoledronic acid (OVX-ZOL-ORAL) or zoledronic acid/Lys-DOCA (1:2) (ZD2) complex as 16 μg/kg zoledronic acid (OVX-ZD2-ORAL) for 12 weeks. Bone mineral density (BMD) and morphological parameter graphs of the SHAM, OVX, OVX-ZOL-IP, OVX-ZOL-ORAL, and OVX-ZD2-ORAL-treated rats after 12 weeks are shown; BMD (a), bone volume fraction (BV/TV, b), and trabecular number (Tb.N, c). Data are presented as mean ± standard deviation ($n = 8$, each). [a] $p < 0.05$ compared with the OVX group; [b] $p < 0.01$ compared with the OVX group; [c] $p < 0.001$ compared with the OVX group; [d] $p < 0.05$ compared with the OVX-ZOL-ORAL group; [e] $p < 0.01$ compared with the OVX-ZOL-ORAL group; [f] $p < 0.001$ compared with the OVX-ZOL-ORAL group. Statistics: two-way ANOVA followed by Tukey's multiple comparison tests.

Table 4
Bone micro-structure parameters of the distal tibiae in rats.

	SHAM	OVX	OVX-ZOL-IP	OVX-ZD2-ORAL	OVX-ZOL-ORAL
BV/TV (%)	62.4 ± 16.2[c,f]	10.2 ± 1.75	30.4 ± 12.0[c,d]	25.5 ± 5.30[b,d]	16.6 ± 0.785
BS/BV (mm^{-1})	16.0 ± 1.61[c,f]	33.2 ± 2.35	33.9 ± 4.65	29.2 ± 2.71[a,e]	34.5 ± 1.25
Tb.Th (μm)	184 ± 41.3[c,f]	114 ± 7.02	109 ± 12.4	133 ± 13.5	112 ± 4.65
Tb.Sp (μm)	143 ± 51.0[c,f]	994 ± 106	254 ± 77.4[c,f]	444 ± 89.4[c,d]	562 ± 41.9[c]
Tb.N (mm^{-1})	3.48 ± 0.305[c,f]	0.897 ± 0.166	2.74 ± 0.743[c,f]	1.93 ± 0.390[c]	1.49 ± 0.060[a]
Tb.Pf (mm^{-1})	−11.8 ± 0.700[c,f]	10.1 ± 1.15	7.83 ± 0.477[c]	6.05 ± 1.05[c,f]	8.85 ± 0.872[a]
SMI	−1.56 ± 0.361[c,f]	2.18 ± 0.097	1.52 ± 0.066[c,f]	1.81 ± 0.091[c,d]	2.04 ± 0.024

Each value represents the mean ± standard deviation ($n = 8$). [a]$p < 0.05$ compared with the OVX group; [b]$p < 0.01$ compared with the OVX group; [c]$p < 0.001$ compared with the OVX group; [d]$p < 0.05$ compared with the OVX-ZOL-ORAL group; [e]$p < 0.01$ compared with the OVX-ZOL-ORAL group; [f]$p < 0.001$ compared with the OVX-ZOL-ORAL group. Statistics: two-way ANOVA followed by Tukey's multiple comparison tests. Abbreviations: SHAM, sham-operated; OVX, ovariectomized; OVX-ZOL-IP, once weekly intraperitoneal injection of 1.6 μg/kg of zoledronic acid; OVX-ZD2-ORAL, once weekly oral administration of ZD2 complex as 16 μg/kg of zoledronic acid; OVX-ZOL-ORAL, once weekly oral administration of 16 μg/kg of zoledronic acid; BV/TV, bone volume fraction; BS/BV, bone surface/volume ratio; Tb.Th, trabecular thickness; Tb.Sp, trabecular separation; Tb.N, trabecular number; Tb.Pf, trabecular pattern factor; SMI, structure model index.

those in the OVX group 12 weeks after treatment. Additionally, the values for F_{max} and stiffness in the OVX-ZD2-ORAL group were 1.42- and 1.29-fold higher than those in the OVX-ZOL-ORAL group, respectively. However, no significant difference in the F_{max} or stiffness was observed between the OVX and OVX-ZOL-ORAL groups.

3.7. Histological evaluation

As seen in the histomorphology of tibiae stained with H&E and TRAP, the trabecular region of the OVX group showed small, thin, and sparse morphology compared with that of the SHAM group, but rats that were given zoledronic acid intra-peritoneally showed a greatly improved trabecular bone structure, with increasing volume and connectivity of the trabeculae (Fig. 6(a)). Compared with the OVX group, the OVX-ZD2-ORAL group also demonstrated thicker and denser microarchitecture in cancellous bone than bones from the OVX or OVX-ZOL-ORAL group, consistent with the μCT images and quantitative data on trabecular bone area. From the osteoclast parameters determined by histomorphometric analysis, the OVX-ZOL-IP and OVX-ZD2-ORAL group showed 60% and 47% lower osteoclast number on trabecular bone surfaces than the OVX control group (16.08 ± 6.83/mm, $p < 0.05$), respectively (Fig. 6(b)).

4. Discussion

In this study, we assessed the possibility of changing the route of administration of zoledronic acid to an oral dosage form and its therapeutic efficacy in an estrogen-deficient osteoporosis rat model. The modification of zoledronic acid with Lys-DCOA resulted in successful oral absorption and indicated sufficient therapeutic effect in the osteoporosis model.

Zoledronic acid is usually administered at a dose of 4 mg IV over >15 min every 3 or 4 weeks for the treatment of hypercalcemia of malignancy, multiple myeloma, and metastatic bone lesions of solid tumors, or a 5 mg infusion once per year for the treatment or prevention of osteoporosis (Li and Davis, 2003). Increasing the dose interval can reduce discomfort but also induces other problems, such as the inability to withdraw or halt the effects of the infused drug due to side effects (Nam et al., 2012). Additionally, too rapid injection of a bisphosphonate can cause complex formation with calcium in the blood, which can then lead to renal failure by being retained in the kidney. Renal deterioration and hypocalcemia, hypophosphatemia, and hypomagnesemia are uncommon but can be issues with zoledronic acid (Bonomi et al., 2010; Perazella and Markowitz, 2008; Rosen et al., 2003). Considering the side effects of the infused drug, oral delivery of zoledronic acid may be beneficial for patients, especially those who need a long-term and chronic care regimen to prevent bone metastasis and osteoporosis.

As mentioned, the major impediment to the successful oral delivery of zoledronic acid is its poor lipophilicity and intestinal membrane permeability, similar to other bisphosphonates. Thus, bisphosphonates should be transported though the epithelial layer via a paracellular pathway. However, all bisphosphonates are expected to be completely ionized and would be negatively charged at physiological pH (6–8) in the small intestine, which further disrupts paracellular transport

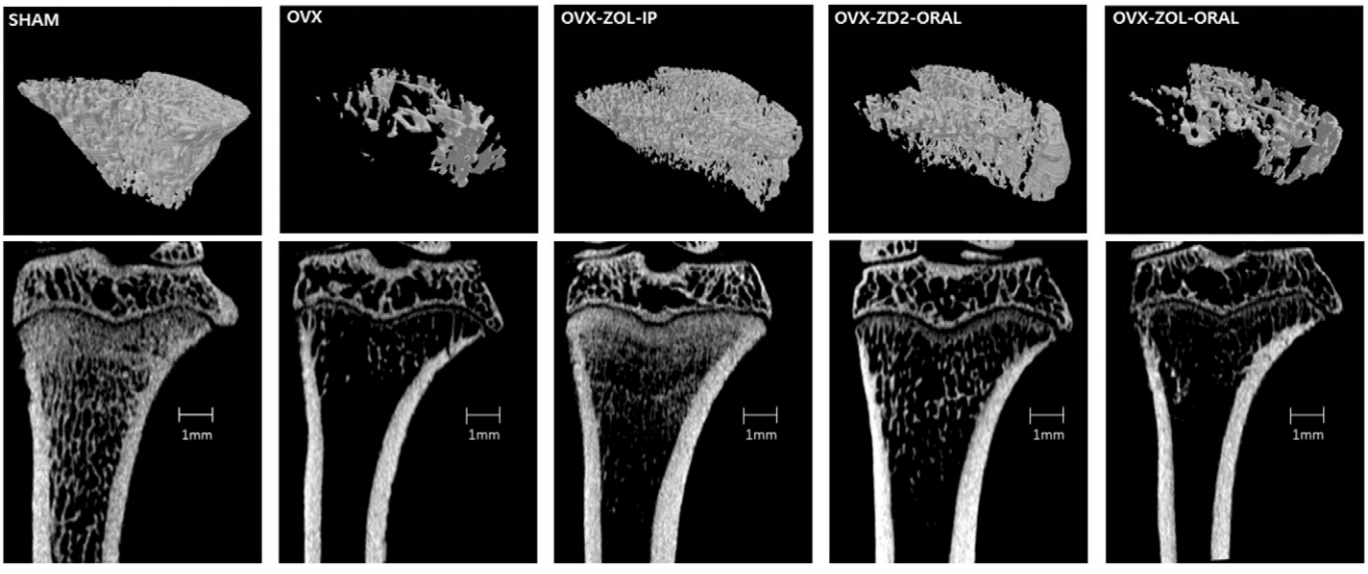

Fig. 4. Representative 2D and 3D images of the distal tibia of SHAM, OVX, OVX-ZOL-IP, OVX-ZOL-ORAL, and OVX-ZD2-ORAL-treated rats ($n = 8$ for each group) at 12 weeks after treatment.

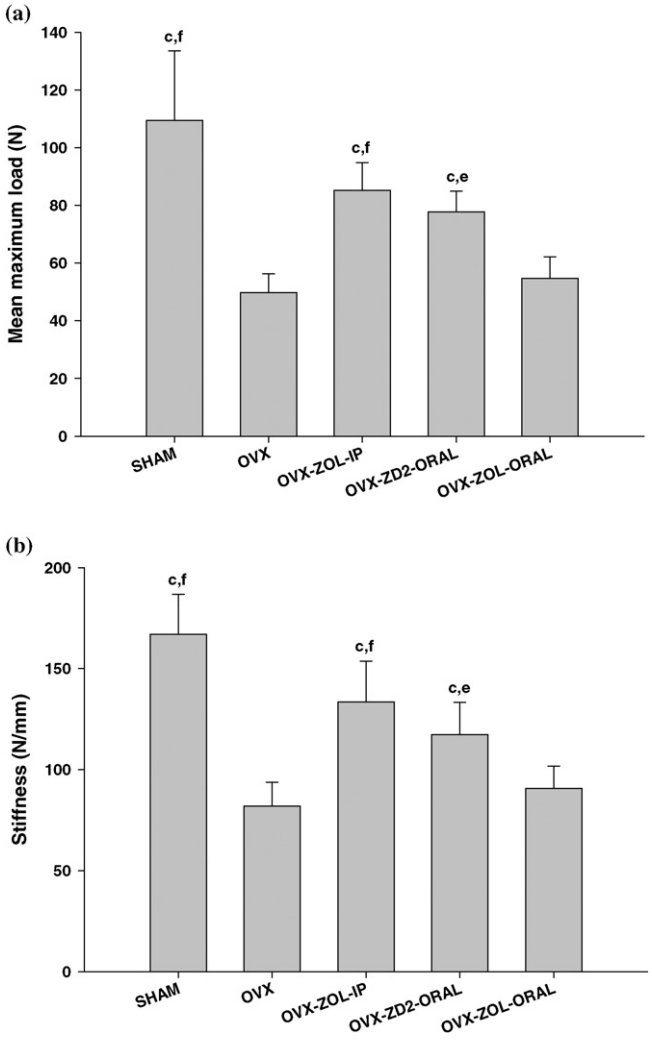

Fig. 5. Bone mechanical properties of tibiae from rats that were either sham-operated (SHAM) or ovariectomized (OVX) and treated with once-weekly intraperitoneal injection of 1.6 μg/kg zoledronic acid (OVX-ZOL-IP), or once-weekly oral administration of 16 μg/kg zoledronic acid (OVX-ZOL-ORAL) or zoledronic acid/Lys-DOCA (1:2) (ZD2) complex as 16 μg/kg zoledronic acid (OVX-ZD2-ORAL) for 12 weeks; ultimate load at failure (F_{max}, a) and stiffness (b) are shown. Data are presented as mean ± standard deviation ($n = 8$, each). [a]$p < 0.05$ compared with the OVX group; [b]$p < 0.01$ compared with the OVX group; [c]$p < 0.001$ compared with the OVX group; [d]$p < 0.05$ compared with the OVX-ZOL-ORAL group; [e]$p < 0.01$ compared with the OVX-ZOL-ORAL group; [f]$p < 0.001$ compared with the OVX-ZOL-ORAL group. Statistics: two-way ANOVA followed by Tukey's multiple comparison tests.

because the brush-border membrane also has a negative charge (Boulenc et al., 1993; Ruifrok and Mol, 1983). Moreover, complex formation with divalent cations in the GI tract can also cause poor absorption (Gertz et al., 1993). To address these limitations, we conjugated Lys-DOCA ionically to the zoledronic acid molecule as an oral absorption enhancer. The ZD complex displayed significantly increased oral bioavailability compared with pure zoledronic acid.

Several modes of action can be suggested for the improvement of polar and hydrophilic active molecule permeation in the presence of Lys-DOCA. First, the DOCA molecule complex with zoledronic acid is formed by ion pairing, thus improving the hydrophilic-lipophilic balance and improving absorption (Hofmann and Mysels, 1988; Miller et al., 2010; Samiei et al., 2014). In this study, the solubility of ZD2 in PBS at pH 6.8 was about 9.5-fold lower than that of zoledronic acid, but its partition coefficient was significantly increased. In previous studies, the amorphous solid dispersion of a poorly water soluble drug has resulted in an increase in the apparent solubility without a decrease in the apparent permeability, leading to successful oral absorption (Dahan et al., 2013; Frank et al., 2012, 2014; Miller et al., 2012)In the same way, the lipophilic property and membrane permeability of zoledronic acid can be enhanced by ion pairing with the hydrophobic DOCA molecule, but the solubility–permeability trade-off does not exist because the zoledronic acid in the complex is present in an amorphous form. Second, changes in mucosal barrier properties, mucus rheology, and membrane fluidity lead to increased diffusion and absorption of zoledronic acid molecule through the membrane because the conjugated DOCA consists of a hydrophobic β-side and a hydrophilic α-side and can act as a surfactant (Aungst, 2000). For these reasons, the in vitro permeability of zoledronic acid through an artificial intestinal membrane or a Caco-2 cell monolayer was significantly improved and the permeability value was increased as the conjugation ratio of Lys-DOCA increased. In addition, the DOCA molecule in the complex might interact with bile acid transporters and act as an adhesive for drug molecules, resulting in an increasing concentration gradient across the membrane (Jeon et al., 2013; Park and Byun, 2014). For these reasons, the ZD complex may show considerably higher intestinal absorption than zoledronic acid; the ZD2 complex had 13.6-fold higher oral bioavailability than zoledronic acid.

Next, we studied whether the oral ZD2 complex had pharmaceutical efficacy in osteoporosis rats in comparison with intra-peritoneal injection of zoledronic acid. The osteoporosis rat model was induced by overiectomy and we then administered zoledronic acid or ZD2 complex once weekly for 12 weeks. The results demonstrated that the BMD in the tibiae and trabecular bone density of tibial bone in OVX rats treated with oral ZD2 complex were improved significantly, compared with the OVX group, and comparable with those given zoledronic acid intraperitoneally. In the microarchitecture of distal tibia trabecular bone using μCT analysis, all parameters, such as BV/TV, BS/BV, Tb/N, and Th.Sp, indicated that the oral ZD2 complex improved bone quality by increasing the volume and connectivity of the trabecular. In particular, the BMD in the tibiae, density of the tibial bone, and trabecular bone morphology and microarchitectural parameters in OVX rats treated with oral ZD2 complex were improved significantly compared with weekly oral administration of free zoledronic acid. Thus, zoledronic acid can be absorbed effectively through the intestinal membrane and exhibit anti-osteoporotic effects by conjugation with Lys-DOCA. However, unlike the other parameters, Tb.Th appeared to be lower in the zoledronic acid and ZD2-treated groups versus the OVX and SHAM groups. Previous studies indicated that lower Tb.Th occurred in the active remodeling process, characterized by increased trabecular numbers and reduced trabecular thickness in the presence of a finer network of more trabeculae (Nam et al., 2012; Sims et al., 2003). Moreover, the ZD2 complex exerted a protective effect on the mechanical properties of bone after ovariectomy, probably due to the improved quality of the material properties of the bone tissue, such as the network of collagen fibrils, and increase in density of the cortical bone.

In the present study, we administered zoledronic acid or the ZD2 complex 2 weeks after ovariectomy to evaluate their anti-osteoporosis effects. In previous in vivo μCT studies, major changes in the proximal tibia of OVX rats were observed within the first three months, especially in the second week postovariectomy, suggesting that anti-resorptive treatment of OVX rats in this early time window is able to preserve the existing architecture after the initiation of estrogen deficiency as well as effectively recover bone mass (Boyd et al., 2006; Brouwers et al., 2008; Campbell et al., 2008; Laib et al., 2001). In addition, this early time point could be analogous to a time window of initiation of anti-resorptive treatment in humans after the onset of menopause (Lane et al., 1999). For these reasons, our results demonstrated not only preventative effects against osteoporosis but also new bone formation in the zoledronic acid injection and oral ZD2 treatment groups. The accumulation of a dense layer of cancellous bone beneath the growth plate was visible at week 14, reflecting the pharmacodynamic effects of zoledronic acid treatment on longitudinal growth during the experiment. However, there are some differences in the results of treatment

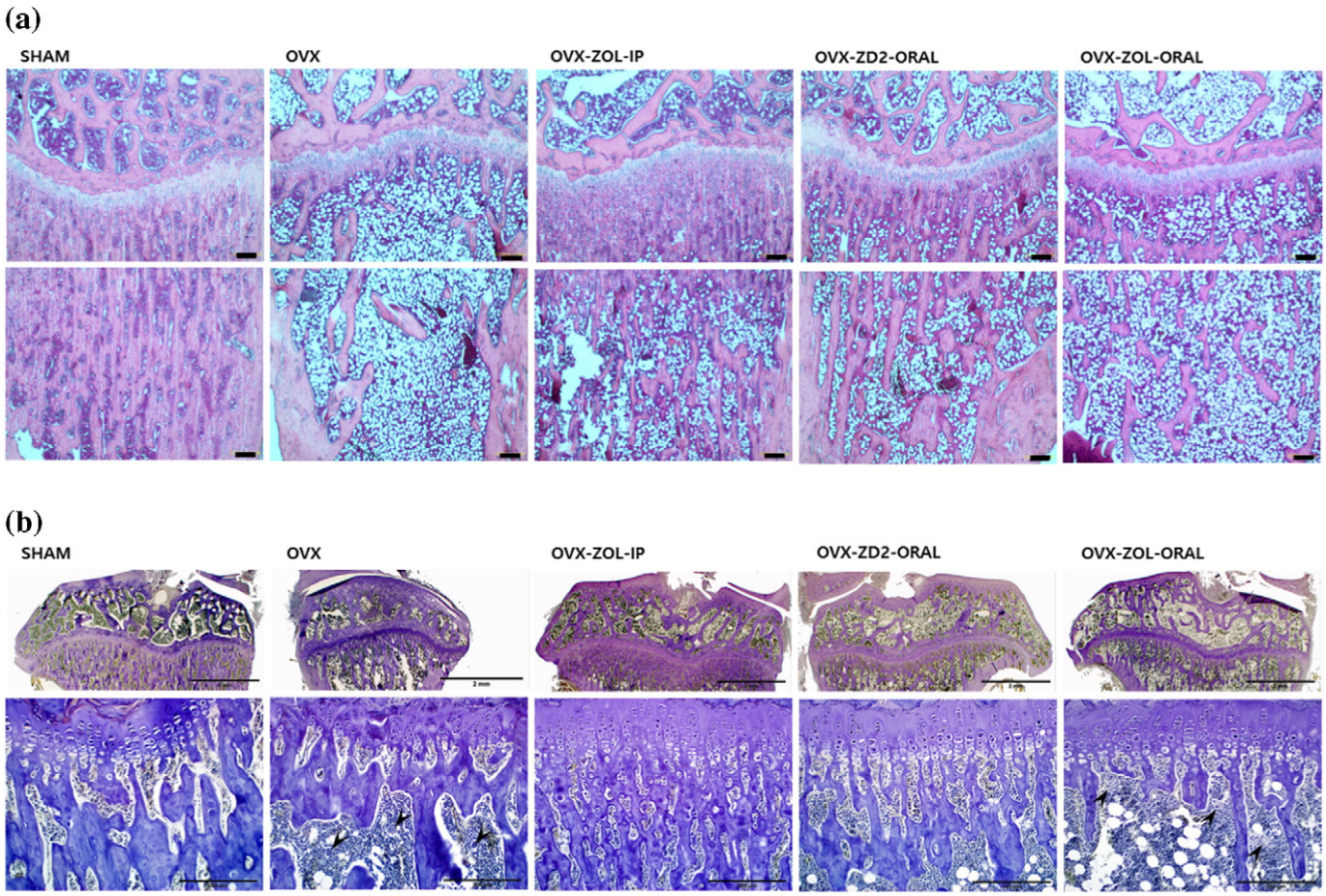

Fig. 6. Representative longitudinal cross-sectional images of proximal rat tibia taken 12 weeks after treatment ($n = 8$ for each group). (a) Staining with hematoxylin and eosin (H&E), scale bar = 200 μm. (b) Staining with tartrate-resistant acid phosphatase (TRAP). Arrows indicate TRAP-positive osteoclasts. Scale bars of upper and lower images represent 2 mm and 200 μm, respectively.

reported by Perilli et al., 2010, with zoledronic acid injected 2 weeks after ovariectomy. In that study, the bone volume fraction in the proximal tibia was approximately 577% higher than that of the OVX group and allowed the bone to be fully restored to initial values and maintained at SHAM control values at 12 weeks after treatment with zoledronic acid. However, in this study, the ovariectomized rats injected with zoledronic acid showed a significantly lower bone volume fraction in the proximal tibia than the SHAM control values at week 12 (initiation of treatment), corresponding to partial bone recovery. This difference might be because a more severe estrogen-deficient osteoporosis was induced at 2 weeks after ovariectomy in comparison with the previous study, suggesting a relatively later initiation of zoledronic acid administration. We also collected the data in a single study on anti-osteoporosis effects in OVX rats, which might represent inconsistent results.

In this study, the ZD2 complex clearly showed better anti-osteoporotic efficacy than zoledronic acid following oral administration; however, the OVX-ZOL-IP group still showed greater improvements in all morphological parameters than the OVX-ZD2-ORAL group. Thus, further studies are needed to determine the most appropriate oral dose regimens for the ZD2 complex corresponding to the conventional injectable form, which is expected to improve patient compliance and therapeutic efficacy as well as expand drug indications, such as the prevention of osteoporosis and bone metastases.

5. Conclusions

Ionic complexation of Lys-DOCA enhanced the lipophilicity of zoledronic acid; this is a key feature for increasing drug permeability across the intestinal membrane. This facilitated active absorption of the ZD2 complex and displayed significantly higher permeability through the artificial intestinal membrane and Caco-2 cell monolayer compared with pure zoledronic acid, which resulted in a 13.6-fold increase in the oral bioavailability of zoledronic acid. Furthermore, the OVX rats treated orally with ZD2 complex showed inhibition of osteoporosis progression and the loss of trabecular microarchitectural parameters in the distal tibia, indicating that the orally absorbed ZD2 complex promoted osteogenesis, thickened trabecular bone, and strengthened trabecular connectivity. Thus, the oral dosage form containing ZD2 complex is expected to improve patient compliance and therapeutic efficacy, replacing the conventional injectable form.

Conflicts of interest

The authors declare no conflicts of interest.

Acknowledgments

This research was supported by the Basic Science Research Program, through the National Research Foundation of Korea (NRF), funded by the Ministry of Science, ICT & Future Planning (NRF-2014R1A1A1003122).

References

Ag, N., Glausch, A., Lohse, O., Mutz, M., Petersen, H., Sigg, J., Vogel, C., Weber, H., 2008. Crystalline forms of zoledronic acid WO2008064849.

Aronhime, J., Revital, L., Pharma, T., 2005. Zoledronic acid crystal forms, zoledronate sodium salt crystal forms, amorphous zoledronate sodium salt, and processes for their preparation WO2005005447.
Aungst, B.J., 2000. Intestinal permeation enhancers. J. Pharm. Sci. 89, 429–442.
Black, D.M., Delmas, P.D., Eastell, R., Reid, I.R., Boonen, S., Cauley, J.A., Cosman, F., Lakatos, P., Leung, P.C., Man, Z., Mautalen, C., Mesenbrink, P., Hu, H., Caminis, J., Tong, K., Rosario-Jansen, T., Krasnow, J., Hue, T.F., Sellmeyer, D., Eriksen, E.F., Cummings, S.R., 2007. Once-yearly zoledronic acid for treatment of postmenopausal osteoporosis. N. Engl. J. Med. 356, 1809–1822.
Blanchette, P.S., Pritchard, K.I., 2015. The role of bisphosphonates in early- and advanced-stage breast cancer: have we finally optimized care? Oncology 29, 23–30.
Boissier, S., Ferreras, M., Peyruchaud, O., Magnetto, S., Ebetino, F.H., Colombel, M., Delmas, P., Delaissé, J.M., Clézardin, P., 2000. Bisphosphonates inhibit breast and prostate carcinoma cell invasion, an early event in the formation of bone metastases. Cancer Res. 60, 2949–2954.
Bonomi, M., Nortilli, R., Molino, A., Sava, T., Santo, A., Caldara, A., Cetto, G.L., 2010. Renal toxicity and osteonecrosis of the jaw in cancer patients treated with bisphosphonates: a long-term retrospective analysis. Med. Oncol. 27, 224–229.
Boulenc, X., Marti, E., Joyeux, H., Roques, C., Berger, Y., Fabre, G., 1993. Importance of the paracellular pathway for the transport of a new bisphosphonate using the human Caco-2 monolayers model. Biochem. Pharmacol. 46, 1591–1600.
Boyd, S.K., Davison, P., Müller, R., Gasser, J.A., 2006. Monitoring individual morphological changes over time in ovariectomized rats by in vivo micro-computed tomography. Bone 39, 854–862.
Brouwers, J.E., Lambers, F.M., Gasser, J.A., van Rietbergen, B., Huiskes, R., 2008. Bone degeneration and recovery after early and late bisphosphonate treatment of ovariectomized wistar rats assessed by in vivo micro-computed tomography. Calcif. Tissue Int. 82, 202–211.
Campbell, G.M., Buie, H.R., Boyd, S.K., 2008. Signs of irreversible architectural changes occur early in the development of experimental osteoporosis as assessed by in vivo micro-CT. Osteoporos. Int. 19, 1409–1419.
Cetin, M., Youn, Y.S., Capan, Y., Lee, K.C., 2008. Preparation and characterization of salmon calcitonin-biotin conjugates. AAPS PharmSciTech 9, 1191–1197.
Corey, E., Brown, L.G., Quinn, J.E., Poot, M., Roudier, M.P., Higano, C.S., Vessella, R.L., 2003. Zoledronic acid exhibits inhibitory effects on osteoblastic and osteolytic metastases of prostate cancer. Clin. Cancer Res. 9, 295–306.
Dahan, A., Beig, A., Ioffe-Dahan, V., Agbaria, R., Miller, J.M., 2013. The twofold advantage of the amorphous form as an oral drug delivery practice for lipophilic compounds: increased apparent solubility and drug flux through the intestinal membrane. AAPS J. 15, 347–353.
Dunford, J.E., Thompson, K., Coxon, F.P., Luckman, S.P., Hahn, F.M., Poulter, C.D., Ebetino, F.H., Rogers, M.J., 2001. Structure-activity relationships for inhibition of farnesyl diphosphate synthase in vitro and inhibition of bone resorption in vivo by nitrogen-containing bisphosphonates. J. Pharmacol. Exp. Ther. 296, 235–242.
Ezra, A., Golomb, G., 2000. Administration routes and delivery systems of bisphosphonates for the treatment of bone resorption. Adv. Drug Deliv. Rev. 31, 175–195.
Frank, K.J., Rosenblatt, K.M., Westedt, U., Hölig, P., Rosenberg, J., Mägerlein, M., Fricker, G., Brandl, M., 2012. Amorphous solid dispersion enhances permeation of poorly soluble ABT-102: true supersaturation vs. apparent solubility enhancement. Int. J. Pharm. 437, 288–293.
Frank, K.J., Westedt, U., Rosenblatt, K.M., Hölig, P., Rosenberg, J., Mägerlein, M., Fricker, G., Brandl, M., 2014. What is the mechanism behind increased permeation rate of a poorly soluble drug from aqueous dispersions of an amorphous solid dispersion? J. Pharm. Sci. 103, 1779–1786.
Gertz, B.J., Holland, S.D., Kline, W.F., Matuszewski, B.K., Porras, A.G., 1993. Clinical pharmacology of alendronate sodium. Osteoporos. Int. 3, S13–S16.
Green, J.R., Müller, K., Jaeggi, K.A., 1994. Preclinical pharmacology of CGP 42'446, a new, potent, heterocyclic bisphosphonate compound. J. Bone Miner. Res. 9, 745–751.
Hofmann, A.F., Mysels, K.J., 1988. Bile salts as biological surfactants. Colloids Surf. 30, 145–173.
Hornby, S.B., Evans, G.P., Hornby, S.L., Pataki, A., Glatt, M., Green, J.R., 2003. Long-term zoledronic acid treatment increases bone structure and mechanical strength of long bones of ovariectomized adult rats. Calcif. Tissue Int. 72, 519–527.
Hubatsch, I., Ragnarsson, E.G., Artursson, P., 2007. Determination of drug permeability and prediction of drug absorption in Caco-2 monolayers. Nat. Protoc. 2, 2111–2119.
Jena, S.K., Singh, C., Dora, C.P., Suresh, S., 2014. Development of tamoxifen-phospholipid complex: novel approach for improving solubility and bioavailability. Int. J. Pharm. 473, 1–9.
Jeon, O.C., Hwang, S.R., Al-Hilal, T.A., Park, J.W., Moon, H.T., Lee, S., Park, J.H., Byun, Y., 2013. Oral delivery of ionic complex of ceftriaxone with bile acid derivative in non-human primates. Pharm. Res. 30, 959–967.
Khajuria, D.K., Razdan, R., Mahapatra, D.R., 2015. Development, in vitro and in vivo characterization of zoledronic acid functionalized hydroxyapatite nanoparticle based formulation for treatment of osteoporosis in animal model. Eur. J. Pharm. Sci. 66, 173–183.
Laib, A., Kumer, J.L., Majumdar, S., Lane, N.E., 2001. The temporal changes of trabecular architecture in ovariectomized rats assessed by MicroCT. Osteoporos. Int. 12, 936–941.
Lane, N.E., Haupt, D., Kimmel, D.B., Modin, G., Kinney, J.H., 1999. Early estrogen replacement therapy reverses the rapid loss of trabecular bone volume and prevents further deterioration of connectivity in the rat. J. Bone Miner. Res. 14, 206–214.
Li, E.C., Davis, L.E., 2003. Zoledronic acid: a new parenteral bisphosphonate. Clin. Ther. 25, 2669–2708.
Lin, J.H., 1996. Bisphosphonates: a review of their pharmacokinetic properties. Bone 18, 75–85.
Merrion Research Ill Ltd., 2010. Solid oral dosage form containing an enhancer. US7704977B2.
Miller, J.M., Dahan, A., Gupta, D., Varghese, S., Amidon, G.L., 2010. Enabling the intestinal absorption of highly polar antiviral agents: ion-pair facilitated membrane permeation of zanamivir heptyl ester and guanidino oseltamivir. Mol. Pharm. 7, 1223–1234.
Miller, J.M., Beig, A., Carr, R.A., Spence, J.K., Dahan, A., 2012. A win-win solution in oral delivery of lipophilic drugs: supersaturation via amorphous solid dispersions increases apparent solubility without sacrifice of intestinal membrane permeability. Mol. Pharm. 9, 2009–2016.
Mohakhud, P.K., Veerender, M., Nandanmudi, K.B., Moses, B., Banerjee, S., 2006. Crystalline form of zoledronic acid US20060178439.
Nam, S.H., Jeong, J.H., Che, X., Lim, K.E., Nam, H., Park, J.S., Choi, J.Y., 2012. Topically administered risedronate shows powerful anti-osteoporosis effect in ovariectomized mouse model. Bone 50, 149–155.
Park, J.W., Byun, Y., 2014. Ionic complex of risedronate with positively charged deoxycholic acid derivative: evaluation of physicochemical properties and enhancement of intestinal absorption in rats. Arch. Pharm. Res. 37, 1560–1569.
Park, J.W., Hwang, S.R., Jeon, O.C., Moon, H.T., Byun, Y., 2013. Enhanced oral absorption of ibandronate via complex formation with bile acid derivative. J. Pharm. Sci. 102, 341–346.
Perazella, M.A., Markowitz, G.S., 2008. Bisphosphonate nephrotoxicity. Kidney Int. 74, 1385–1393.
Perilli, E., Le, V., Ma, B., Salmon, P., Reynolds, K., Fazzalari, N.L., 2010. Detecting early bone changes using in vivo micro-CT in ovariectomized, zoledronic acid-treated, and sham-operated rats. Osteoporos. Int. 21, 1371–1382.
Rosen, L.S., Gordon, D., Kaminski, M., Howell, A., Belch, A., Mackey, J., Apffelstaedt, J., Hussein, M.A., Coleman, R.E., Reitsma, D.J., Chen, B.L., Seaman, J.J., 2003. Long-term efficacy and safety of zoledronic acid compared with pamidronate disodium in the treatment of skeletal complications in patients with advanced multiple myeloma or breast carcinoma: a randomized, double-blind, multicenter, comparative trial. Cancer 98, 1735–1744.
Ruifrok, P.G., Mol, W.E., 1983. Paracellular transport of inorganic and organic ions across the rat ileum. Biochem. Pharmacol. 32, 637–640.
Samiei, N., Shafaati, A., Zarghi, A., Moghimi, H.R., Foroutan, S.M., 2014. Enhancement and in vitro evaluation of amifostine permeation through artificial membrane (PAMPA) via ion pairing approach and mechanistic selection of its optimal counter ion. Eur. J. Pharm. Sci. 51, 218–223.
Sims, N.A., Dupont, S., Krust, A., Clement-Lacroix, P., Minet, D., Resche-Rigon, M., Gaillard-Kelly, M., Baron, R., 2003. Deletion of estrogen receptors reveals a regulatory role for estrogen receptors-beta in bone remodeling in females but not in males. Bone 30, 18–25.
Spernath, A., Aserin, A., Ziserman, L., Danino, D., Garti, N., 2007. Phosphatidylcholine embedded microemulsions: physical properties and improved o. J. Control. Release 119, 279–290.
Stenberg, P., Norinder, U., Luthman, K., Artursson, P., 2001. Experimental and computational screening models for the prediction of intestinal drug absorption. J. Med. Chem. 44, 1927–1937.
Thar Pharmaceuticals, Inc., 2011. Novel oral forms of a phosphonic acid derivative WO2011014781.
Ziemba, A., Hayes, E., Freeman 3rd, B.B., Ye, T., Pizzorno, G., 2011. Development of an oral form of azacytidine: 2'3'5'triacetyl-5-azacytidine. Chemother. Res. Pract. 2011, 965826.
Zometa® [package insert], 2003. East Hanover. Novartis Pharmaceutical Corp., NJ.